Electronic Research Archive

http://www.aimspress.com/journal/era

ERA, 31(4): 1840–1862.
DOI: 10.3934/era.2023095
Received: 30 November 2022
Revised: 15 January 2023
Accepted: 28 January 2023
Published: 08 February 2023

Research article

A novel adaptive event-triggered reliable H_∞ control approach for networked control systems with actuator faults

Xingyue Liu[1,2], Kaibo Shi[1,3,4,5,*], Yiqian Tang[1], Lin Tang[1], Youhua Wei[4] and Yingjun Han[6]

[1] School of Electronic Information and Electrical Engineering, Chengdu University, Chengdu 610106, China

[2] Key Laboratory of Intelligent Manufacturing Quality Big Data Tracing and Analysis of Zhejiang Province, China Jiliang University, Hangzhou 310018, China

[3] Engineering Research Center of Power Quality of Ministry of Education, Anhui University, Hefei 230601, China

[4] Geomathematics Key Laboratory of Sichuan Province, Chengdu University of Technology, Chengdu 610059, China

[5] Data Recovery Key Laboratory of Sichuan Province, College of Mathematics and Information Science, Neijiang Normal University, Neijiang 641100, China

[6] China Tobacco Sichuan Industrial Co. LTD Chengdu Cigarette Factory, Chengdu 610066, China

* **Correspondence:** Email: skbs111@163.com.

Abstract: In this paper, a reliable H_∞ control approach under a novel adaptive event-triggering mechanism (AETM) considering actuator faults for networked control systems (NCSs) is addressed. Firstly, the actuator faults are described by a series of independent stochastic variables obeying a certain probability distribution. Secondly, a novel AETM is presented. The triggering threshold can be dynamically adjusted according to the fluctuating trend of the current sampling state, resulting in saving more limited network resources while preserving good control performance. As a result, considering the packet dropout and packet disorder caused by the communication network, the sampling-data model of NCSs with AETM and actuator faults is constructed. Thirdly, by removing the involved auxiliary function and replacing it with a sequence of integrals only related to the system state, a novel integral inequality can be used to reduce conservatism. Thus, a new stability criterion and an event-triggered reliable H_∞ controller design approach can be obtained. Finally, the simulation results are presented to verify the progressiveness of our proposed approach.

Keywords: reliable H_∞ control approach; adaptive event triggering mechanism; actuator faults; networked control systems; stability criterion

1. Introduction

Over the past few decades, the control issues of NCSs have attracted the attention of many researchers, where physical processes, actuators, and sensors are linked together over communication networks [1]. Significant research has been conducted on its wide application in a variety of potential fields, such as unmanned vehicles [2–4], load frequency control (LFC) system [5–8], internet of things and smart power grid.

Communication resources have proved to be increasingly important for control implementations as the medium of data transmission. As a result, many studies are bending their efforts to save communication bandwidth and reduce communication load [9–12]. The event-triggering control mechanism (ETM) has received more and more attention in the control engineering fields [13–19]. The ETM performs its control behavior as needed and is superior to stochastic and periodic sampling mechanisms, which can cause less occupied communication bandwidth. In recent years, some significant advanced achievements with regard to ETM have been discussed in many research findings, such as [5–7, 13, 14, 20–24]. The security control problem of NCSs is addressed in [25], which proposes a novel resilient event-triggering strategy considering the uncertainty of triggering conditions caused by DoS attacks. An event-triggering scheme for NCSs is put forward in [26], where the sampling data will not be transmitted through the communication networks unless a predesigned threshold condition is violated. An ETM for multi-area power systems is proposed in [27]. It is worth noting that the triggering parameter in the general ETM is a constant, independent of the system fluctuation state. To conserve as much communication bandwidth as possible, the AETM with adaptive triggering conditions is widely studied [6,7,28–30]. A dynamically triggering algorithm for multi-areas power systems is designed by [6]. The triggering parameter is no longer constant but adjusted with the change of system state, which can effectively reduce the number of data packets. The main purpose of [7] is to develop an adaptive event-triggering control algorithm for the multi-area LFC system over a limited bandwidth communication channel. Dong et al. [28] puts forward a new event-triggering control architecture for LFC systems with adaptive dynamic programming (ADP). A novel dynamic AETM is proposed in [29], which is flexible enough because the threshold condition is variable for the system state. With the presence of hybrid attacks, a new dynamic-memory event-triggered H_∞ LFC method is established in [30]. The ETM is an effective method to occupy less communication bandwidth and reduce the computational burden of the control system. Appropriate triggering parameters can decide the performance of an ETM design. It motivates us to design an ETM with an adaptive triggering threshold associated with the system state.

NCSs [31–33] are also widely used in a variety of applications ranging from industrial control to critical infrastructure such as power systems, transportation systems, and water supply systems. In fact, the combination of cyber and physical systems will bring some threats to the security of NCSs, such as actuator faults, packet dropout/disorder brought from cyber attacks, physical devices or human actions. Hence, it is very important to design a reliable controller for improving the security of NCSs that can resist and revive failures. There have been many published achievements with regard to reliable controller design. Wang et al. [32] discuss the reliable H_∞ and passive control for NCSs under an adaptive event-triggered scheme with actuator faults and randomly occurring nonlinear perturbations. The robust reliable control problem for uncertain networked control systems is fully investigated in [33]. Li et al. [34] study the problem of stochastic reliable control for NCSs subjected to actuator

failure and input saturation. From the above-published works, it is necessary to design a reliable control approach considering the failures caused by the communication network. Thus, how to design a reliable controller against actuator failures considering AETM is another motivation for this work.

There are some kinds of controller techniques to face the control system, such as predictor-observer based control techniques [35], multi-rate control solutions [36], gain scheduling control methods [37] and H_∞ methods. To accurately estimate and account for the "total disturbance" in uncertain systems with sensor delay, the extended state predictor observer (ESPO)-based active disturbance rejection control (ADRC) is first developed in [35]. A periodic event-triggered system that is susceptible to external disturbance and sensor noise is discussed in [36] along with a systematic non-uniform multi-rate estimation and control framework. The gain-scheduling control strategy is discussed in [37] for an experimental setup featuring a flexible beam, whose stiffness varies with its length. Among the above control theories and methods, H_∞ theory and methods are the most widely used and have received a lot of attention in engineering [6, 7, 24, 32]. When the mathematical model differs from the actual controlled object, the H_∞ controller can keep system performance within acceptable limits. An event-triggered load frequency control for a multi-area power system is investigated in [6] by setting the H_∞ control performance index. The stability and stabilization criteria are studied in [7] to balance the required communication resources and the desired H_∞ control performance. The event-triggered parameters and the memory H_∞ LFC controller gains are obtained simultaneously by a sufficient stabilization criterion in [24]. In [32], the mixed H_∞ and passive control for NCSs under AETM with actuator faults and nonlinear external disturbances have been investigated for the first time. These efforts inspire us to conduct research on the reliable H_∞ control approach, considering actuator faults and AETM for NCSs.

The goal of this paper is to develop a novel event-triggered reliable H_∞ control approach for NCSs using AETM while accounting for actuator faults. The main contributions of this paper are listed as follows:

1) Firstly, a novel AETM has been developed that dynamically adjusts the triggering threshold according to the fluctuating trend of the current sampling state. However, the triggering parameter of ETM is a constant in [23, 26, 27]. Our proposed AETM is a more general case compared with other published ETMs like [23, 26, 27].

2) Moreover, a set of independent stochastic variables varying in $[0, \varpi]$ are modeled to describe the randomly occurring actuator faults. Hence, the sampling-data model of NCSs with AETM and actuator faults is built considering packet dropout and packet disorder caused by the communication network.

3) Furthermore, the less conservative conditions for the asymptotically stable of NCSs and event-triggered reliable H_∞ controller approach are obtained by adopting a novel integral inequality. It is composed by a sequence of integrals only related to the system state, which removes the involved auxiliary function. Finally, the same simulation results can verify the progressiveness of our proposed control method.

4) Finally, through case simulation, the superiority of the proposed AETM in reducing the consumption of network resources is proved under the premise of ensuring the stability of the system. At the same time, it is proved that the proposed event-triggered reliable H_∞ control approach can still guarantee the H_∞ stability of the system under certain actuator faults. The method proposed in this paper can also be applied to other industrial control network systems to achieve less network bandwidth occupancy and anti-interference ability against actuator faults.

The remainder of this work is organized as follows. The adaptive event-triggering mechanism, the sampling-data model of NCSs considering AETM and actuator faults, and H_∞ control objectives are described in Section 2. The main results are shown in Section 3, which are H_∞ stability conditions and the event-triggering H_∞ reliable controller design under AETM. In Section 4, a simulation example is applied to prove the progressiveness of the proposed reliable control method under the AETM for NCSs. The last Section 5 concludes this work.

Notation: Let $\mathbb{R}$, $\mathbb{R}^n$, $\mathbb{R}^{n*m}$ denotes the set of real numbers, the n-dimensional Euclidean space, the set of all $n \times m$ real matrices, respectively; P^{-1} and P^T denote the inverse and transpose of a given matrix P, respectively; $P > 0$ stands for that the matrix P is a real symmetric positive definite matrix; $diag\{\dots\}$ represents a block-diagonal matrix; $\mathbb{E}[.]$ represents the expectation of random variable; $*$ in the matrix represents the symmetry of matrix; $\mathcal{L}_2[0, \infty)$ denotes the space of all square-suable vectors function over $[0, \infty)$.

2. Preliminaries

In this section, the event triggering control framework considering actuator faults and the proposed AETM under our control objectives is presented.

2.1. Continuous-time model of NCSs

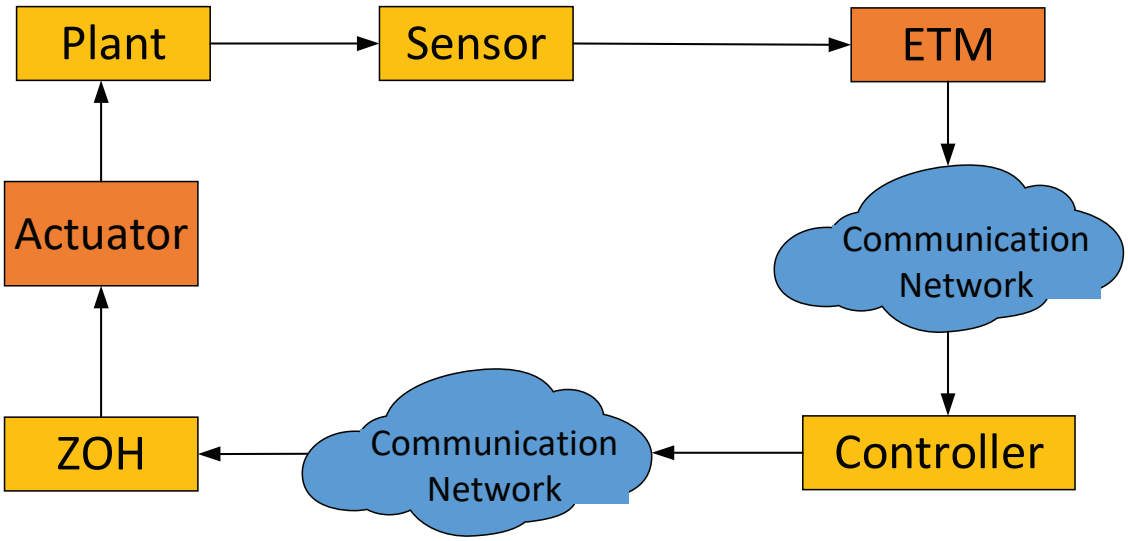

Figure 1. Diagram of NCSs under ETM.

A state-space expression of NCS is proposed in Figure 1 considering exogenous disturbance can be listed as follows:

$$\begin{cases} \dot{x}(t) = Ax(t) + A_d u^w(t) + B\Delta w(t), \\ y(t) = Cx(t) + Du^w(t). \end{cases} \tag{2.1}$$

Where $x(t) \in \mathbb{R}^n$, $u^w(t) \in \mathbb{R}^m, \Delta w(t) \in \mathcal{L}_2[0,\infty)$, $y(t) \in \mathbb{R}^l$ denotes state, controlled input, disturbance input and control output vector respectively; Constant matrices with compatible dimensions are denoted by the symbols A, A_d, B, C, and D. $x(t_0) = x_0$ represents the initial condition for system (2.1). The NCS is controlled over a communication network by a network state feedback controller, which is shown in Figure 1. In order to simplify the analysis, the delays from ETM to Controller and from Controller to Actuator are considered as the total communication delay τ.

2.2. Adaptive event-triggering mechanism

Firstly, the traditional ETM, which is also introduced in [23, 26, 27], is listed as follows:

$$t_{k+1}h = t_k h + \min_{m\in\mathbb{N}}\{mh \mid e^T(l_m h)\Phi e(l_m h) \geq \kappa x^T(t_k h)\Phi x(t_k h)\}. \tag{2.2}$$

Where $t_k h, k \in \mathbb{R}$ denotes the latest transmitted instant determined by ETM, $l_m h = t_k h + mh, m \in \mathbb{R}$ means the sampling instant by sensor. Φ is a positive-definite matrix, $e(l_m h) = x(l_m h) - x(t_k h)$, and κ is a preselected constant.

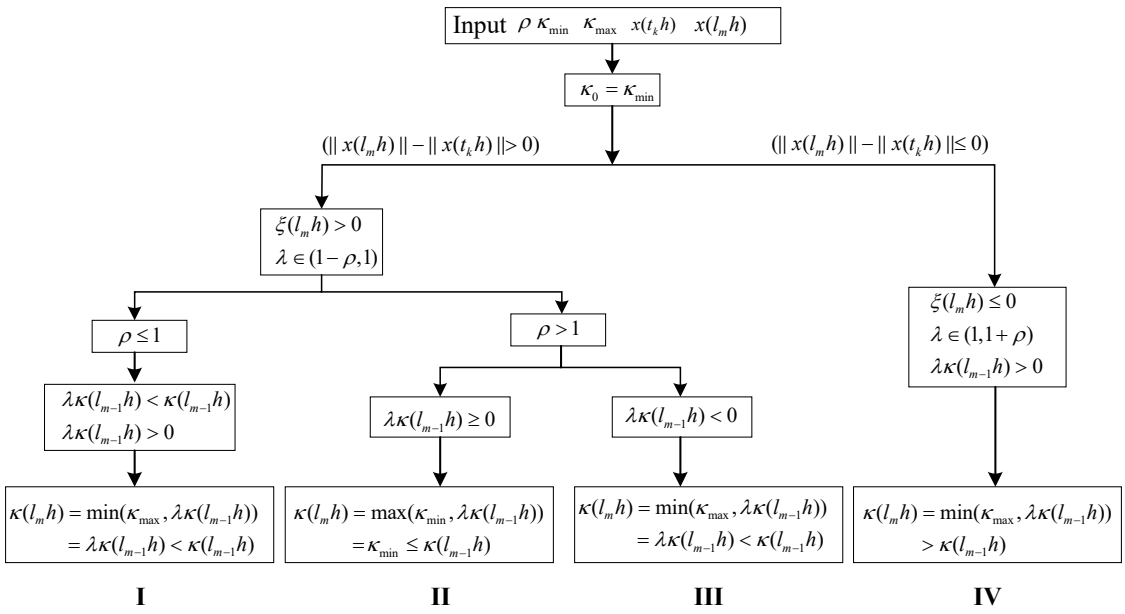

Figure 2. The dynamic change logic block diagram of $\kappa(l_m h)$.

Compared with the time-triggered mechanism, ETM (2.2) can effectively reduce the occupation of communication bandwidth, owing to the occurrence of a transmission depends on a state-dependent threshold. In other words, the sampling data will only be sent if a certain threshold is broken. Nevertheless, it can be seen from those corresponding simulation results that there are still many transmitting packets over the communication networks even if the system is stable. We hope that when the system is well controlled, the number of transmitted packets will be reduced. From this point of view, the preselected parameter κ should be set as an adaptive value adjusted based on the latest transmitted data and current sampled data. Based on the above supposition, the advanced AETM is proposed as follows:

$$t_{k+1}h = t_k h + \min_{m\in\mathbb{N}}\{mh \mid e^T(l_m h)\Phi e(l_m h) \geq \kappa(l_m h)x^T(t_k h)\Phi x(t_k h)\}. \tag{2.3}$$

Where dynamic parameter $\kappa(l_m h)$ is determined by

$$\kappa(l_m h) = \begin{cases} min(\kappa_{max}, \lambda\kappa(l_{m-1}h)) & if \quad \lambda\kappa(l_{m-1}h)) \geq 0, \\ max(\kappa_{min}, \lambda\kappa(l_{m-1}h)) & otherwise. \end{cases} \tag{2.4}$$

Where dynamic parameter $\kappa(l_m h)$ changes with every sampling instant. $\kappa(l_{(m-1)}h) = \kappa(t_k h + (m-1)h)$ means the last dynamic parameter in the last sampling instant $l_{(m-1)}h$. $\lambda = 1 - \frac{2\rho}{\pi} atan(\xi(l_m h)), \xi(l_m h) = \frac{\|x(l_m h)\| - \|x(t_k h)\|}{\|x(t_k h)\|}$. ρ is a positive integer. $atan(.)$ is the arctangent function. It's obvious that $[\kappa_{min}, \kappa_{max}]$ is the bound of $\kappa(l_m h)$, where $\kappa_{min}, \kappa_{max}$ are both positive integer. $\kappa(0) = \kappa_{min}$ is the initial value of $\kappa(l_m h)$. The dynamic change logic of $\kappa(l_m h)$ is shown in Figure 2.

Remark 1: The arctangent function atan(.) is monotonically increasing over its domain $(-\infty, \infty)$, and the range of atan(.) is $(-\frac{\pi}{2}, \frac{\pi}{2})$. $\kappa(l_m h)$ is dynamically adjusted in each sampling instant based on the fluctuating trend of the current sampling state. As shown in Figure 2, if the absolute value of the current sampling state is greater than the absolute value of the recently transmitted state ($\| x(l_m h) \| - \| x(t_k h) \| > 0$), it indicates that the current state is far from the equilibrium point ($x(t) = 0$). Then $\xi(l_m h) > 0$ and $\lambda \in (1-\rho, 1)$ with ρ being a positive integer. According to Eq (2.4), if $\rho \leq 1$, then $\lambda\kappa(l_{m-1}h)) < \kappa(l_{m-1}h)$ and $\lambda\kappa(l_{m-1}h)) > 0$, so $\kappa(l_m h)) = min(\kappa_{max}, \lambda\kappa(l_{m-1}h)) = \lambda\kappa(l_{m-1}h) < \kappa(l_{m-1}h)$, which is presented as the situation of I in Figure 2. If $\rho > 1$, then $\lambda\kappa(l_{m-1}h))$ maybe negative. If $\lambda\kappa(l_{m-1}h))$ is positive, $\kappa(l_m h)) = min(\kappa_{max}, \lambda\kappa(l_{m-1}h)) = \lambda\kappa(l_{m-1}h) < \kappa(l_{m-1}h)$, which is presented as the situation of II in Figure 2. And if $\kappa(l_m h)$ is negative, $\kappa(l_m h) = max(\kappa_{min}, \lambda\kappa(l_{m-1}h)) = \kappa_{min}$, which is presented as the situation of III in Figure 2. In the above three situations, denoted as I, II, and III in Figure 2, a smaller $\kappa(l_m h)$ is set for higher transmission frequency when compared to the latest sampling dynamic parameter $\kappa(l_m h)$. In contrary, when the absolute value of current sampling state is smaller than that of the latest transmitted state larger ($\| x(l_m h) \| - \| x(t_k h) \| \leq 0$), the system tends to be more stable. Then $\xi(l_m h) \leq 0$, $\lambda \in (1, 1+\rho)$ and $\lambda\kappa(l_{m-1}h)) > 0$, then $\kappa(l_m h)) = min(\kappa_{max}, \lambda\kappa(l_{m-1}h)) = \lambda\kappa(l_{m-1}h) > \kappa(l_{m-1}h)$, which is presented as the situation of IV in Figure 2. In this case, when compared to the latest sampling dynamic parameter $\kappa(l_{m-1}h)$, the larger $\kappa(l_m h)$ is used for a lower communication frequency, saving more communication bandwidth. Noting that when $\kappa(l_m h)$ iterates with the fluctuation of every sampling system state, κ_{min} and κ_{max} are the lower and upper bounds of $\kappa(l_m h)$. In summary, compared with the general ETM like [23, 26, 27] with a constant threshold, the threshold can be dynamically adjusted as the fluctuating trend of the current sampling state in every sampling instant in our proposed AETM (2.3).

Remark 2: According to the definition of Eq (2.4), the value of $\kappa(l_m h)$ is limited by $[\kappa_{min}, \kappa_{max}]$. When $\kappa_{min} = \kappa_{max} = 0$, the proposed AETM (2.3) can reduce to traditional time triggering mechanism. When $\kappa_{min} \neq 0$ and $\rho = 0$, the proposed AETM (2.3) will degrade to the general ETM like [23, 26, 27] with a constant threshold. Thus, the proposed AETM is a more general case compared with other published ETMs [23, 26, 27, 38–40].

2.3. Sampling-data model of NCSs considering AETM and actuator faults

The transmission process of signals is presented in Figure 3. It can be seen from Figure 3 that the time triggering mechanism is adopted by the sensor with sampling sequence $\mathcal{S}_1 = 0, h, 2h, \ldots, kh, k \in \mathbb{R}$ like [38]. When the triggering condition is violated, the AETM transmits the selected sampling data $x(t_k h)$. The triggering transmission sequence set is expressed as $\mathcal{S}_2 = t_1 h, t_2 h, \ldots, t_k h, k \in \mathbb{R}$.

Considering the packet dropout and packet disorder in the communication network, the sequence set of control signals successfully arrived at the actuator is shown as $\mathcal{S}_3 = t_1, t_2, \ldots, t_k, k \in \mathbb{R}$. Apparently, there is $\mathcal{S}_3 \in \mathcal{S}_2 \in \mathcal{S}_1$.

It can be seen from Figure 3, the sampling data $x(t_k h)$ selected to transmission by AETM is transmitted to the controller, which forms the control output. And from Figure 3, the actuators receive control actions from controller as follows:

$$u(t) = Kx(t_k h), t \in [t_k, t_{k+1}). \tag{2.5}$$

And the update period of the actuator is related to the trigger period of the AETM, the network communication delay, and the number of packet dropout/disorder, which will lead to the uncertainty of the update period of the actuator. The derivation of the update period of actuator T_k is as follows:

$$T_k = t_{k+1} - t_k = t_{k+1+\gamma} h + \tau_{k+1+\gamma} - (t_k h + \tau_k), \quad T_k \in [T_1, T_2], \quad k = 0, 1, 2, \ldots\ldots \tag{2.6}$$

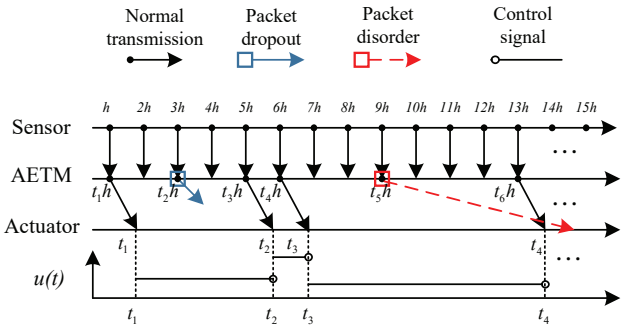

Figure 3. The transmission process of signal.

Where γ denotes the continuous count of packet dropout/disoder caused by network transmission. Different k leads to different T_k, indicating the uncertainty of T_k. T_1 and T_2 denote the minimum and maximum of T_k.

Meanwhile, taking the random failures of actuators in NCSs into account, it is assumed that:

$$u^W(t) = Fu(t) = diag\{f_1(t), f_2(t), \ldots, f_m(t)\}u(t). \tag{2.7}$$

There are m independent random variables $f_s(t)(s = 1, 2, \ldots, m)$, where $f_s(t)$ is an independent random variable that varies in the range of $[0, \varpi]$. ϖ denotes a constant and $\varpi \geq 1$. The expectation and variance of $f_s(t)$ are assumed to be expressed by $\bar{f}_s$ and δ^2_{fs}, respectively. Thus, the following definition can be obtained:

$$\begin{aligned} &\bar{F} = \mathbb{E}(F) = diag\{\mathbb{E}(f_1), \mathbb{E}(f_2), \ldots, \mathbb{E}(f_m)\} = diag\{\bar{f}_1, \bar{f}_2, \ldots, \bar{f}_m\} = \sum_{s=1}^{m} \bar{f}_s I_s \\ &I_s = diag\{0_{(s-1)}, 1, 0_{m-s}\}. \end{aligned} \tag{2.8}$$

$\bar{F}$ denotes the expectation of F.

Defining $\mathcal{U}_l = [t_k, t_{k+1})$, the system delay version can be built for the every two update instants of actuator in front and rear by defining $\tau(t) = t - t_k h$. Then $\dot{\tau}(t) = 1$, $\tau(t) \in [\tau_m, \tau_M], \tau_M > \tau_m$. $\tau_m = \underline{\tau}$ denotes the minimum of communication network delay, and $\tau_M = \bar{\tau} + \bar{\gamma} + \bar{T}_{kh}$, where $\bar{\tau}$, $\bar{\gamma}$, $\bar{T}_{kh}$ denotes the maximum of communication network delay, the maximum of continuous count of packet dropout/disoder, the maximum triggering period of AETM respectively.

Combining (2.1), (2.5), (2.7) and (2.8), the sampling-data model of NCSs considering AETM and actuator faults can be constructed as follows:

$$\begin{cases} \dot{x}(t) = Ax(t) + A_d\bar{F}Kx(t-\tau(t)) + A_d(F-\bar{F})Kx(t-\tau(t)) + B\Delta w(t), \\ y(t) = Cx(t) + D\bar{F}K(t-\tau(t)) + D(F-\bar{F})K(t-\tau(t)), \quad t \in \mathcal{U}_l. \end{cases} \tag{2.9}$$

2.4. Control objective

Taking the external disturbances into consideration, an appropriate controller is designed considering actuator failures like Eq (2.7) under the AETM (2.3) while guaranteeing a stable performance. In detail, the following two states should be ensured.

1) The system (2.9) is asymptotically stable with H_∞ performance when there are no external disturbances, $\Delta w(t) = 0$.

2) When $\Delta w(t) \in \mathcal{L}_2[0, \infty)$, there is a positive scalar γ such that $\| y(t) \| \leq \gamma \| \Delta w(t) \|_2$ holds under the zero initial condition.

2.5. Main lemma

Before deriving the stability criteria, Lemma1 should be introduced.

Lemma 1 [41]: For a given matrix $Z > 0$ and a differentiable function $x(.) : [a, b] \to \mathbb{R}^n$, the following inequality holds:

$$-\int_a^b \dot{x}^T(s)Z\dot{x}(s)ds \leq -\sum_{l=0}^{r} \frac{\nu_l}{b-a}(\Xi_l(a,b))^T Z(\Xi_l(a,b)), \tag{2.10}$$

where

$$\Xi_l(a,b) = \begin{cases} x(b) - x(a), & l = 0 \\ \sum_{k=0}^{l} f_{lk}x(b) - f_{l0}x(a) - \sum_{k=1}^{l} \frac{f_{lk}k!}{(b-a)^k}\mathcal{F}^k_{(a,b)}x(t), & l \geq 1 \end{cases},$$

$$\nu_l = \left(\sum_{k=0}^{l} \frac{f_{lk}}{l+k+1}\right)^{-1}, \quad f_{lk} = \begin{cases} 1, & k = l, \quad l \geq 0 \\ -\sum_{v=k}^{l-1} c(lv)f_{vk}, & k = 0, 1 \ldots, l-1, \quad l \geq 1 \end{cases},$$

and $c_{lv} = \sum_{j=0}^{v} \frac{f_{vj}}{l+j+1} / \sum_{j=0}^{v} \frac{f_{vj}}{v+j+1}$. The multiple integral terms with degree $k = 1, 2, \ldots, r$ are denoted as

$$\mathcal{F}^k_{(a,b)}x(t) = \begin{cases} \int_a^b x(s)ds, & k = 1. \\ \int_a^b \int_{s_1}^b \cdots \int_{s_{k-1}}^b x(s_k)ds_k \ldots ds_2 ds_1, & k > 1. \end{cases}$$

Remark 3: Setting $r = 0, r = 1, r = 2$ separately, for example, Eq (2.10) can be transformed into the Jensen inequality [42], the Wirtinger-based inequality [43], and the auxiliary function based inequality [44]. Applying integer r to regulate computation accuracy and complexity synchronously. It can be seen that Eq (2.10) estimates the integral quadratic form $\int_a^b \dot{x}^T(s)Zx(s)ds$ without conservatism by setting a relatively large r. At the same time, more decision variables are introduced inevitably by increasing r, resulting in computational complexity. In other word, owing to the adjustability of r, the trade-off between computational accuracy and complexity will be obtained in Lemma 1.

3. H_∞ stability performance analysis and H_∞ reliable controller design

The main results are shown in this section, which are the H_∞ stability condition and the H_∞ reliable event-triggering controller design approach under AETM.

3.1. H_∞ stability performance analysis

The robust H_∞ performance analysis for NCSs considering actuator failures and AETM is presented in Theorem1.

Theorem 1. The system (2.9) is asymptotically stable with a H_∞ norm bound γ for some given parameters τ_m, τ_M, and $\delta_{fs}(s = 1, \ldots, m)$, if there exist positive definite matrices P, Q_1, Q_2, Φ, R_1, R_2, Z, such that the following inequality holds:

$$\Omega = \begin{bmatrix} \Omega_1 + \Omega_{10} & \Omega_2 & \Omega_4 & \Omega_6 \\ * & \Omega_3 & 0 & 0 \\ * & * & \Omega_5 & 0 \\ * & * & * & \Omega_7 \end{bmatrix} < 0, \tag{3.1}$$

where $\Omega_3 = diag[-R_1^{-1}, -R_2^{-1}, -Z^{-1}, -I]$, $\Omega_5 = diag[\widetilde{R}_1, \widetilde{R}_2, \widetilde{Z}]$, $\widetilde{R}_1 = diag\{\underbrace{-R_1^{-1}}_{m}\}$, $\widetilde{R}_2 = diag\{\underbrace{-R_2^{-1}}_{m}\}$, $\widetilde{Z} = diag\{\underbrace{-Z^{-1}}_{m}\}$, $\Omega_7 = diag\{\underbrace{I}_{m}\}$.

$$\Omega_2 = \begin{bmatrix} \tau_m A^T & (\tau_M - \tau_m)A^T & \tau_m A^T & C^T \\ 0 & 0 & 0 & 0 \\ \tau_m K^T \bar{F}^T A_d^T & (\tau_M - \tau_m)K^T \bar{F}^T A_d^T & \tau_m K^T \bar{F}^T A_d^T & K^T \bar{F}^T D^T \\ 0 & 0 & 0 & 0 \\ \vdots & \vdots & \vdots & \vdots \\ \tau_m B^T & (\tau_M - \tau_m)B^T & \tau_m B^T & 0 \end{bmatrix}, \quad \Omega_6 = \begin{bmatrix} 0 & \ldots & 0 \\ 0 & \ldots & 0 \\ \delta_{f1} D I_1 K & \ldots & \delta_{fm} D I_m K \\ 0 & \ldots & 0 \\ \ldots & \ldots & \ldots \\ 0 & \ldots & 0 \end{bmatrix},$$

$$\Omega_4 = \begin{bmatrix} 0 & \ldots & 0 & 0 & \ldots & 0 & 0 & \ldots & 0 \\ 0 & \ldots & 0 & 0 & \ldots & 0 & 0 & \ldots & 0 \\ \tau_m \delta_{f1} A_d I_1 K & \ldots & \tau_m \delta_{fm} A_d I_m K & (\tau_M - \tau_m)\delta_{f1} A_d I_1 K & \ldots & (\tau_M - \tau_m)\delta_{fm} A_d I_m K & \tau_M \delta_{f1} A_d I_m K & \ldots & \tau_M \delta_{fm} A_d I_m K \\ 0 & \ldots & 0 & 0 & \ldots & 0 & 0 & & \\ \ldots & \ldots & \ldots & \ldots & \ldots & \ldots & \ldots & \ldots & \ldots \\ 0 & \ldots & 0 & 0 & \ldots & 0 & 0 & \ldots & 0 \end{bmatrix}.$$

The element in Ω_{10} is just $\vartheta_{12.12} = -\gamma^2$, and the elements $\varphi_{ij}(i, j = 1, 2 \ldots 12)$ in Ω_1 are listed as

following:

$$\varphi_{1.1} = PA + A^T P^T + Q_1 - 9R_1 - \frac{\pi^2}{4}Z, \quad \varphi_{1.2} = -2R_1, \quad \varphi_{1.3} = PA_d\bar{F}K + \frac{\pi^2}{4}Z, \quad \varphi_{1.5} = -24R_1,$$
$$\varphi_{1.6} = 60R_1, \quad \varphi_{1.12} = PB, \quad \varphi_{2.2} = -4R_1 - 9R_2 - Q_1 + Q_2, \quad \varphi_{2.3} = 3R_2, \quad \varphi_{2.5} = 36R_1,$$
$$\varphi_{2.6} = -60R_1, \quad \varphi_{2.9} = -24R_2, \quad \varphi_{2.10} = 60R_2, \quad \varphi_{3.3} = -\frac{\pi^2}{4}Z - 18R_2 + \kappa_{min}\Phi, \quad \varphi_{3.4} = 3R_2,$$
$$\varphi_{3.7} = -24R_2, \quad \varphi_{3.8} = 60R_2, \quad \varphi_{3.9} = 36R_2, \quad \varphi_{3.10} = -60R_2, \quad \varphi_{4.4} = -9R_2 - Q_2, \quad \varphi_{4.7} = 36R_2,$$
$$\varphi_{4.8} = -60R_2, \quad \varphi_{5.5} = -192R_1, \quad \varphi_{5.6} = 360R_1, \quad \varphi_{6.6} = -720R_1, \quad \varphi_{7.7} = -192R_2, \quad \varphi_{7.8} = 360R_2,$$
$$\varphi_{8.8} = -720R_2, \quad \varphi_{9.9} = -192R_2, \quad \varphi_{9.10} = 360R_2, \quad \varphi_{10.10} = -720R_2, \quad \varphi_{11.11} = -\Phi.$$

Proof: At first, the following Lyapunov-Krasovskii functional (LKF) candidates are considered.

$$V(t) = \sum_{i=1}^{4} V_i(t), \tag{3.2}$$

where

$$V_1(t) = x^T(t)Px(t),$$
$$V_2(t) = \int_{t-\tau_m}^{t} x^T(s)Q_1x(s)ds + \int_{t-\tau_M}^{t-\tau_m} x^T(s)Q_2x(s)ds,$$
$$V_3(t) = \int_{t-\tau_m}^{t} \tau_m(s-t+\tau_m)\dot{x}^T(s)R_1\dot{x}(s)ds + \int_{t-\tau_M}^{t-\tau_m} (\tau_M-\tau_m)(s-t+\tau_M-\tau_m)\dot{x}^T(s)R_2\dot{x}(s)ds,$$
$$V_4(t) = \tau_M^2 \int_{t_kh}^{t} \dot{x}^T(s)Z\dot{x}(s)ds - \frac{\pi^2}{4}\int_{t_kh}^{t} [x(s) - x(t_kh)]^T Z[x(s) - x(t_kh)]ds.$$

Considering that the state space model (2.9) of the system contains random variable F, we can get the expectation of derivative for $V(t)$ as:

$$
\begin{aligned}
\mathbb{E}\{\dot{V}_1(t)\} &= \mathbb{E}\{2x^T(t)P\dot{x}(t)\} = 2x^T(t)P(Ax(t) + A_d\bar{F}Kx(t-\tau(t)) + B\Delta w(t)),\\
\mathbb{E}\{\dot{V}_2(t)\} &= x^T(t)Q_1x(t) - x^T(t-\tau_m)(Q_1-Q_2)x(t-\tau_m) - x^T(t-\tau_M)Q_2x(t-\tau_M),\\
\mathbb{E}\{\dot{V}_3(t)\} &= \mathbb{E}\{\tau_m^2\dot{x}^T(t)R_1\dot{x}(t) + (\tau_M-\tau_m)^2\dot{x}^T(t)R_2\dot{x}(t)\\
&\quad - \tau_m\int_{t-\tau_m}^{t}\dot{x}^T(s)R_1\dot{x}(s)ds - (\tau_M-\tau_m)\int_{t-\tau_M}^{t-\tau_m}\dot{x}^T(s)R_2\dot{x}(s)ds\}\\
&= \sum_{s=1}^{m}\bar{\delta}_{fs}^2x^T(t-\tau(t))(A_dI_sK)^T(\tau_m^2R_1 + (\tau_M-\tau_m)^2R_2)(A_dI_sK)x(t-\tau(t))\\
&\quad - \mathbb{E}\{\tau_m\int_{t-\tau_m}^{t}\dot{x}^T(s)R_1\dot{x}(s)ds - (\tau_M-\tau_m)\int_{t-\tau_M}^{t-\tau_m}\dot{x}^T(s)R_2\dot{x}(s)ds\} + \bar{A}(\tau_m^2R_1 + (\tau_M-\tau_m)^2R_2)\bar{A},\\
\mathbb{E}\{\dot{V}_4(t)\} &= \mathbb{E}\{\tau_M^2\dot{x}^T(t)Z\dot{x}(t)\} - \frac{\pi^2}{4}[x(t)-x(t-\tau(t))]^TZ[x(t)-x(t-\tau(t))]\\
&= \bar{A}(\tau_m^2Z)\bar{A} + \sum_{s=1}^{m}\bar{\delta}_{fs}^2x^T(t-\tau(t))(A_dI_sK)^T(\tau_m^2Z)(A_dI_sK)x(t-\tau(t)).
\end{aligned}
\tag{3.3}
$$

Where $\bar{A} = Ax(t) + A_d\bar{F}Kx(t-\tau(t)) + B\Delta w(t)$. By setting $r = 2$, the Lemma1 can be used to deal with the integral terms in $\dot{V}_3(t)$, as shown below:

$$
\begin{aligned}
-\mathbb{E}\{\tau_m\int_{t-\tau_m}^{t}\dot{x}^T(s)R_1\dot{x}(s)ds\} &\le \mathbb{E}\{-\nu_0\Theta_0^TR_1\Theta_0 - \nu_1\Theta_1^TR_1\Theta_1 - \nu_2\Theta_2^TR_1\Theta_2\}\\
&= -\nu_0\Theta_0^TR_1\Theta_0 - \nu_1\Theta_1^TR_1\Theta_1 - \nu_2\Theta_2^TR_1\Theta_2,
\end{aligned}
\tag{3.4}
$$

$$
\begin{aligned}
-\mathbb{E}\{(\tau_M-\tau_m)\int_{t-\tau_M}^{t-\tau_m}\dot{x}^T(s)R_2\dot{x}(s)ds\} &\le \mathbb{E}\{-(\tau_M-\tau(t))\int_{t-\tau_M}^{t-\tau(t)}\dot{x}^T(s)R_2\dot{x}(s)ds\\
&\quad - (\tau(t)-\tau_m)\int_{t-\tau(t)}^{t-\tau_m}\dot{x}^T(s)R_2\dot{x}(s)ds\}\\
&\le \mathbb{E}\{-\nu_0\Theta_3^TR_2\Theta_3 - \nu_1\Theta_4^TR_2\Theta_4 - \nu_2\Theta_5^TR_2\Theta_5\\
&\quad - \nu_0\Theta_6^TR_2\Theta_6 - \nu_1\Theta_7^TR_2\Theta_7 - \nu_2\Theta_8^TR_2\Theta_8,\}\\
&= -\nu_0\Theta_3^TR_2\Theta_3 - \nu_1\Theta_4^TR_2\Theta_4 - \nu_2\Theta_5^TR_2\Theta_5\\
&\quad - \nu_0\Theta_6^TR_2\Theta_6 - \nu_1\Theta_7^TR_2\Theta_7 - \nu_2\Theta_8^TR_2\Theta_8,
\end{aligned}
\tag{3.5}
$$

where $\nu_i(i = 0, 1, 2)$ can be obtained from (2.10), and

$$
\begin{aligned}
&\Theta_0 = \varepsilon_1(t) - \varepsilon_2(t), \quad \Theta_1 = \frac{1}{2}\varepsilon_1(t) + \frac{1}{2}\varepsilon_2(t) - \varepsilon_3(t), \quad \Theta_2 = \frac{1}{6}\varepsilon_1(t) - \frac{1}{6}\varepsilon_2(t) + \varepsilon_3(t) - 2\varepsilon_4(t),\\
&\Theta_3 = \varepsilon_5(t) - \varepsilon_6(t), \quad \Theta_4 = \frac{1}{2}\varepsilon_5(t) + \frac{1}{2}\varepsilon_6(t) - \varepsilon_7(t), \quad \Theta_5 = \frac{1}{6}\varepsilon_5(t) - \frac{1}{6}\varepsilon_6(t) + \varepsilon_7(t) - 2\varepsilon_8(t),\\
&\Theta_6 = \varepsilon_2(t) - \varepsilon_5(t), \quad \Theta_7 = \frac{1}{2}\varepsilon_2(t) + \frac{1}{2}\varepsilon_5(t) - \varepsilon_9(t), \quad \Theta_8 = \frac{1}{6}\varepsilon_2(t) - \frac{1}{6}\varepsilon_5(t) + \varepsilon_9(t) - 2\varepsilon_{10}(t),
\end{aligned}
$$

where

$$\varepsilon_1(t) = x(t), \quad \varepsilon_2(t) = x(t-\tau_m), \quad \varepsilon_3(t) = \frac{1}{\tau_m}\int_{t-\tau_m}^{t} x(s)ds, \quad \varepsilon_4(t) = \frac{1}{\tau_m^2}\int_{t-\tau_m}^{t}\int_{s}^{t} x(\theta)d\theta ds,$$
$$\varepsilon_5(t) = x(t-\tau(t)), \quad \varepsilon_6(t) = x(t-\tau_M), \quad \varepsilon_7(t) = \frac{1}{\tau_M-\tau(t)}\int_{t-\tau_M}^{t-\tau(t)} x(s)ds,$$
$$\varepsilon_8(t) = \frac{1}{(\tau_M-\tau(t))^2}\int_{t-\tau_M}^{t-\tau(t)}\int_{s}^{t} x(\theta)d\theta ds, \quad \varepsilon_9(t) = \frac{1}{\tau(t)-\tau_m}\int_{t-\tau(t)}^{t-\tau_m} x(s)ds,$$
$$\varepsilon_{10}(t) = \frac{1}{(\tau(t)-\tau_m)^2}\int_{t-\tau(t)}^{t-\tau_m}\int_{s}^{t} x(\theta)d\theta ds.$$

Defining

$$\zeta^T(t) = [\varepsilon_1(t), \quad \varepsilon_2(t), \quad \varepsilon_5(t), \quad \varepsilon_6(t), \quad \varepsilon_3(t), \quad \varepsilon_4(t), \quad \varepsilon_7(t), \quad \varepsilon_8(t), \quad \varepsilon_9(t), \quad \varepsilon_{10}(t), \quad e(l_m h), \quad \Delta w(t)].$$

Considering the AETM condition (2.3), the following inequality can be obtained:

$$e^T(l_m h)\Phi e(l_m h) - \kappa(l_m h)x^T(t-\tau(t))\Phi x(t-\tau(t)) < 0 \tag{3.6}$$

Therefore, considering (2.10)–(3.6) together, the following inequality can be obtained as:

$$\begin{aligned}\mathbb{E}\{\dot{V}(t)\} \leq & \zeta^T(t)[\Omega_1 + \Pi_1^T(\tau_m^2 R_1 + \tau_M^2 Z + (\tau_M-\tau_m)^2 R_2)\Pi_1 \\ & + \sum_{s=1}^{m}\delta_{fs}^2 e_3^T(A_d I_s K)^T(\tau_m^2 R_1 + \tau_M^2 Z + (\tau_M-\tau_m)^2 R_2)(A_d I_s K)e_3]\zeta(t).\end{aligned} \tag{3.7}$$

Where Ω_1 has been defined in (3.1) and $\Pi_1 = Ae_1 + A_d\bar{F}Ke_3 + Be_{12}, \quad e_i = [0_{n\times(i-1)n} I_n 0_{n\times(12-i)n}]$.

Following that, the robust H_∞ performance of the system (2.9) in the presence of external disturbance should be considered. The following inequality can be established:

$$\mathbb{E}\{\dot{V}(t)\} + \mathbb{E}\{y^T(t)y(t)\} - \gamma^2\Delta w^T(t)\Delta w(t) < 0. \tag{3.8}$$

$\mathbb{E}\{\dot{V}(t)\} \leq -\mathbb{E}\{\| y(t) \|$ can be derived from (3.8) with $\Delta w(t) = 0$. That is to say $\mathbb{E}\{\dot{V}(t)\} < 0$. The positive definite matrices P, Q_1, Q_2, Φ, R_1, R_2, Z make $V(t) > 0$. It means that the energy function $V(t)$ containing the system state gradually tends to 0 with the advance of time. The system (2.9) is asymptotically stable when the external disturbance is 0 (with $\Delta w(t) = 0$).

Owing to $\mathbb{E}\{\dot{V}(t)\}$ is continuous in t, taking integration both side of (3.8) from 0 to $+\infty$, we can derive that

$$\mathbb{E}\{V(+\infty)\} - \mathbb{E}\{V(0)\} < \int_0^{+\infty}(\mathbb{E}\{-y^T(t)y(t)\} + \gamma^2\Delta w^T(t)\Delta w(t))dt. \tag{3.9}$$

Due to the initial condition $\mathbb{E}\{V(0)\} = 0$ and $V(t) > 0$, inequality (Eq 3.9) is equivalent to $\int_0^{+\infty}(\mathbb{E}\{-y^T(t)y(t)\} + \gamma^2\Delta w^T(t)\Delta w(t))dt > 0$. Furthermore $\| y(t) \|_2 \leq \gamma \| \Delta w(t) \|_2$ can be obtained. As a result, system (2.9) is asymptotically stable and has a H_∞ performance.

Equation (3.8) can be expressed as:

$$\mathbb{E}\{\dot{V}(t)\} + \mathbb{E}\{y^T(t)y(t)\} - \gamma^2\Delta w^T(t)\Delta w(t) = \zeta^T(t)\mathbb{X}\zeta(t) < 0. \tag{3.10}$$

That is to say $\mathbb{X} < 0$, where:

$$\begin{aligned}\mathbb{X} =&\Omega_1 + \Omega_{10} + \Pi_1^T(\tau_m^2 R_1 + \tau_M^2 Z + (\tau_M - \tau_m)^2 R_2)\Pi_1 + \Pi_2^T\Pi_2 \\ &+ \sum_{s=1}^{m} \delta_{fs}^2 e_3^T (A_d I_s K)^T (\tau_m^2 R_1 + \tau_M^2 Z + (\tau_M - \tau_m)^2 R_2)(A_d I_s K)e_3 + \sum_{s=1}^{m} \delta_{fs}^2 e_3^T (DI_s K)^T (DI_s K)e_3 < 0.\end{aligned} \tag{3.11}$$

Thus, the inequality (Eq 3.11) can be transformed into inequality (Eq 3.1) based on Schur complement.

There is $\Pi_2 = Ce_1 + D\bar{F}Ke_3$. And Ω_1, Ω_2, Ω_3, Ω_4, Ω_5, Ω_6, Ω_7, Ω_{10} have been presented in Theorem 1.

3.2. H_∞ controller design

While it can be seen from $\varphi_{1.3} = PA_d\bar{F}K + \frac{\pi^2}{4}Z$ in Ω_1, the multiplication of two unknown variables K and P make matrix inequality (Eq 3.1) nonlinear and the controller gain K cannot be solved by LMI tool of Matlab. The purpose of this paper is to solve the event-triggered reliable H_∞ controller gain K. Theorem 2 is an extension of Theorem 1. The nonlinear inequality (Eq 3.1) in Theorem 1 is processed into linear inequality (Eq 3.12) in Theorem 2. Through the LMI tool of MATLAB, the controller gain K can be obtained by Theorem 2.

Theorem 2. The system (2.9) is asymptotically stable with a H_∞ norm bound γ for some given parameters $\tau_m, \tau_M, \delta_{fs}(s = 1, \ldots, m)$, if there exist positive definite matrices X, $\bar{Q}_1$, $\bar{Q}_2$, $\bar{\Phi}$, $\bar{R}_1$, $\bar{R}_2$, $\bar{Z}$, such that the following inequality holds:

$$\Omega = \begin{bmatrix} \bar{\Omega}_1 + \Omega_{10} & \bar{\Omega}_2 & \bar{\Omega}_4 & \bar{\Omega}_6 \\ * & \bar{\Omega}_3 & 0 & 0 \\ * & * & \bar{\Omega}_5 & 0 \\ * & * & * & \Omega_7 \end{bmatrix} < 0, \tag{3.12}$$

where $\bar{\Omega}_3 = diag\{\bar{R}_1 - 2X, \ \bar{R}_2 - 2X, \ \bar{Z} - 2X, \ -I\}$, $\bar{\Omega}_5 = diag\{\widehat{R_1}, \ \widehat{R_2}, \ \widehat{Z}\}$, $\widehat{R_1} = diag\{\underbrace{\bar{R}_1 - 2X}_{m}\}, \widehat{R_2} = diag\{\underbrace{\bar{R}_2 - 2X}_{m}\}, \widehat{Z} = diag\{\underbrace{\bar{Z} - 2X}_{m}\}$.

$$\bar{\Omega}_2 = \begin{bmatrix} \tau_m A^T & (\tau_M - \tau_m)A^T & \tau_m A^T & C^T \\ 0 & 0 & 0 & 0 \\ \tau_m Y^T \bar{F}^T A_d^T & (\tau_M - \tau_m)Y^T \bar{F}^T A_d^T & \tau_m Y^T \bar{F}^T A_d^T & Y^T \bar{F}^T D^T \\ 0 & 0 & 0 & 0 \\ \vdots & \vdots & \vdots & \vdots \\ \tau_m B^T & (\tau_M - \tau_m)B^T & \tau_m B^T & 0 \end{bmatrix}, \quad \bar{\Omega}_6 = \begin{bmatrix} 0 & \ldots & 0 \\ 0 & \ldots & 0 \\ \delta_{f1} DI_1 Y & \ldots & \delta_{fm} DI_m Y \\ 0 & \ldots & 0 \\ \ldots & \ldots & \ldots \\ 0 & \ldots & 0 \end{bmatrix},$$

$$\bar{\Omega}_4 = \begin{bmatrix} 0 & \ldots & 0 & 0 & \ldots & 0 & 0 & \ldots & 0 \\ 0 & \ldots & 0 & 0 & \ldots & 0 & 0 & \ldots & 0 \\ \tau_m \delta_{f1} A_d I_1 Y & \ldots & \tau_m \delta_{fm} A_d I_m Y & (\tau_M - \tau_m)\delta_{f1} A_d I_1 Y & \ldots & (\tau_M - \tau_m)\delta_{fm} A_d I_m Y & \tau_M \delta_{f1} A_d I_1 Y & \ldots & \tau_M \delta_{fm} A_d I_m Y \\ 0 & \ldots & 0 & 0 & \ldots & 0 & 0 & & \\ \ldots & \ldots & \ldots & \ldots & \ldots & \ldots & \ldots & \ldots & \ldots \\ 0 & \ldots & 0 & 0 & \ldots & 0 & 0 & \ldots & 0 \end{bmatrix}.$$

The elements $\varphi_{ij}(i, j = 1, 2 \ldots 12)$ in $\bar{\Omega}_1$ are listed as following:

$$\varphi_{1.1} = XA^T + AX + \bar{Q}_1 - 9\bar{R}_1 - \frac{\pi^2}{4}\bar{Z}, \quad \varphi_{1.2} = -2\bar{R}_1, \quad \varphi_{1.3} = BY + \frac{\pi^2}{4}\bar{Z}, \quad \varphi_{1.5} = -24\bar{R}_1,$$
$$\varphi_{1.6} = 60\bar{R}_1, \quad \varphi_{1.12} = B, \quad \varphi_{2.2} = -4\bar{R}_1 - 9\bar{R}_2 - \bar{Q}_1 + \bar{Q}_2, \quad \varphi_{2.3} = 3\bar{R}_2, \quad \varphi_{2.5} = 36\bar{R}_1,$$
$$\varphi_{2.6} = -60\bar{R}_1, \quad \varphi_{2.9} = -24\bar{R}_2, \quad \varphi_{2.10} = 60\bar{R}_2, \quad \varphi_{3.3} = -\frac{\pi^2}{4}\bar{Z} - 18\bar{R}_2 + \kappa_{min}\bar{\Phi}, \quad \varphi_{3.4} = 34R_2,$$
$$\varphi_{3.7} = -24\bar{R}_2, \quad \varphi_{3.8} = 60\bar{R}_2, \quad \varphi_{3.9} = 36 \quad \bar{R}_2, \varphi_{3.10} = -60 \quad \bar{R}_2, \varphi_{4.4} = -9\bar{R}_2 - \bar{Q}_2, \varphi_{4.7} = 36\bar{R}_2,$$
$$\varphi_{4.8} = -60\bar{R}_2, \quad \varphi_{5.5} = -192\bar{R}_1, \quad \varphi_{5.6} = 360\bar{R}_1, \quad \varphi_{6.6} = -720\bar{R}_1, \quad \varphi_{7.7} = -192\bar{R}_2, \quad \varphi_{7.8} = 360\bar{R}_2,$$
$$\varphi_{8.8} = -720\bar{R}_2, \quad \varphi_{9.9} = -192\bar{R}_2, \quad \varphi_{9.10} = 360\bar{R}_2, \quad \varphi_{10.10} = -720\bar{R}_2, \quad \varphi_{11.11} = -\bar{\Phi},$$

the element in Ω_{10} is just $\vartheta_{12.12} = -\gamma^2$.

Proof: Define $X = P^{-1}$, $\bar{Q}_i = XQ_iX, (i = 1, 2)$, $\bar{\Phi} = X\Phi X$, $\bar{R}_i = XR_iX(i = 1, 2)$, $\bar{Z} = XZX$ and $Y = KX$. The inequality (Eq 3.12) can be obtained from pre- and post- multiplying both sides of (3.1) by $diag\{\underbrace{X}_{11}, I, \underbrace{X}_{3}, I, \underbrace{X}_{3m}, \underbrace{I}_{m}\}$. The non-linear terms in (3.12) can be estimated by the fact of $-HG^{-1}H \leq G - 2H$ for appropriate matrices like [25]. And after the above processing, the nonlinear term $PA_d\bar{F}K$ (with two unknown variables P and K) in $\varphi_{1.3}$ of Ω_1 in LMI (3.1) will become $XPA_d\bar{F}KX = P^{-1}PA_d\bar{F}KP^{-1} = A_d\bar{F}KX$. Making $Y = KX$, the nonlinear term $XPA_d\bar{F}KX$ will become the linear term $A_d\bar{F}Y$ (with only one unknown variables Y). At the same time, PA in LMI (3.1) will become $XPAX = P^{-1}PAP^{-1} = AX$. Therefore, all nonlinear terms become linear terms. Using the LMI toolbox in MATLAB, all unknown variables can be solved, including Y and X. Thus $K = YX^{-1}$ will be obtained.

Remark 4: Theorems 1 and 2 are time-varying due to the characteristic of $\kappa(l_mh)$ changing dynamically at every sampling instant. Because the arctangent function atan(.) varies with time. It is a challenge to analyze control system stability and obtain controller gain. Because $\kappa(l_mh)$ varies in (κ_min, κ_max), when Theorem 1 is used to analyze the H_∞ performance stability and Theorem 2 is used to obtain the controller gain with a given H_∞ performance index, the time-varying $\kappa(l_mh)$ can be substituted with κ_min for less conservatism.

4. Illustrative example

A simulation example is applied to prove the progressiveness of the proposed control method under the AETM in this section.

The pendulum example illustrated in [25, 38] is listed as follows:

$$\dot{x}(t) = \begin{bmatrix} 0 & 1 & 0 & 0 \\ 0 & 0 & \frac{mg}{M} & 0 \\ 0 & 0 & 0 & 1 \\ 0 & 0 & \frac{g}{l} & 0 \end{bmatrix} x(t) + \begin{bmatrix} 0 \\ \frac{1}{M} \\ 0 \\ -\frac{mg}{Ml} \end{bmatrix} u(t) + \begin{bmatrix} 1 \\ 1 \\ 1 \\ 1 \end{bmatrix} \Delta w(t).$$

Where $M = 10$, $m = 1$, $l = 3$, $g = 10$ denotes the cart mass, the pendulum bob mass, the length of the pendulum arm and the gravitational acceleration respectively. The initial state is $x(0) = [0.98, \quad 0, \quad 0.2, \quad 0]^T$ as [25]. $\gamma = 200$, $\tau_m = 0.01$ $\kappa_{min} = 0.005$, $\kappa_{max} = 0.1$ and

$\Delta w(t) = 0.01 sin(2\pi t)$ are set. And making $F = I$ means the actuator is healthy. The corresponding feedback controller and triggering matrix are achieved as:

$$K = [-22.8582 \quad -37.4262 \quad 48.5428 \quad 9.5980],$$
$$\bar{\Phi} = 10^3 * \begin{bmatrix} 2.4244 & -0.0058 & -0.0106 & -0.0318 \\ -0.0058 & 2.4952 & 0.0106 & -0.0591 \\ -0.0106 & 0.0106 & 2.0546 & 0.0284 \\ -0.0318 & -0.0591 & 0.0284 & 2.3584 \end{bmatrix}.$$

It can be seen from Remark 2, if $\kappa_{min} \neq 0, \rho = 0$, the proposed AETM reduces to a general ETM with a constant triggering parameter. Noting that time-triggering is adopted by the sensor in Figure 2 with a trigged period of $h = 0.1$, the sampling period of AETM is $h = 0.1$. On this basis, the average triggering intervals (ATIs) calculated by our proposed AETM when $\rho = 0, \rho = 0.8$ are listed in Table 1 and compared to the results in [6, 25, 38].

Remark 5: It is worth noting that the security control problem of NCSs is investigated by [25] under the DoS attack. The ATI of three cases: no DoS attack, a probabilistic DoS attack, and the worst DoS attack are all calculated and shown in [25]. Thus, the ATI of [25] in Table 1 refers to the case of no DoS attack, which is also considered in this work. Meanwhile, the triggering parameters in [25] and [38] are all set as constants, which are unaffected by system state fluctuations. However, in AETM (2.3), the triggering parameter $\kappa(l_m h)$ is set as a dynamic adjustment value based on system state fluctuation. When the system state fluctuates severely, the control signal will be transmitted frequently. When the system state is well controlled, the control signal should be reduced dynamically. Additionally, the triggering parameter in [6] is set as a dynamic adjustment value rather than a constant. The dynamic adjustment mechanism of [6] is different from the method in this work.

Table 1. ATIs by adopting different ETM.

Triggering mechanisms	[25]	[38]	[6]	$\rho = 0$	$\rho = 0.8$
ATI	0.2115	0.30	1.475	0.4	1.77

When compared to the results in [25] and [38] in Table 1, our proposed AETM can improve ATI regardless of $\rho = 0, \rho = 0.8$. Setting $\rho = 0$, the AETM reduces to $t_{k+1}h = t_k h + \min_{m\in\mathbb{N}}\{mh \mid e^T(l_m h)\Phi e(l_m h) \geq \kappa_{min} x^T(t_k h)\Phi x(t_k h)\}$ like the traditional ETM [23, 26, 27]. $\kappa(l_m h)$ is always κ_{min}, indicating that it always transmits data at a high frequency. Setting $\rho \neq 0$ indicates a faster change rate speed of $\kappa(l_m h)$. $\kappa(l_m h)$ can be dynamically adjusted more flexible as the distance between the current state and the latest transmitted state, resulting in a better average interval. From Table 1, the ATI of $\rho = 0.8$ is larger than $\rho = 0$. Furthermore, even after reducing the proposed AETM to traditional ETM, the ATI is still better than the results in [25] and [38], because the proposed Theorem 1 derived from Lemma 1 is less conservative than those in [25] and [38]. Moreover, the setting of the sensitivity parameter ρ in the proposed ATEM (2.3) enables us to dynamically adjust the trigger effect, which is not considered by AETM in [6]. It can be seen that when $\rho = 0.8$, the ATI is better than that in [6], which illustrates the effect of reducing network bandwidth occupancy is better than the AETM in [6]. Therefore, compared with the AETM in [6], the proposed AETM (2.3) is more flexible.

When the actuator meets a partial failure and $\bar{f}_1 = 0.95$, $\delta_{f1}^2 = 0.05$ is set, the system state responses by setting $\rho = 0$, $\rho = 0.8$ are shown in Figures 4 and 5. It can be seen from Figures 4 and 5 that when ETM with $\rho = 0$, or $\rho = 0.8$ is used, even if encountering a certain degree of actuator fault, the system state converges to zero with good performance under our proposed reliable H_∞ control method.

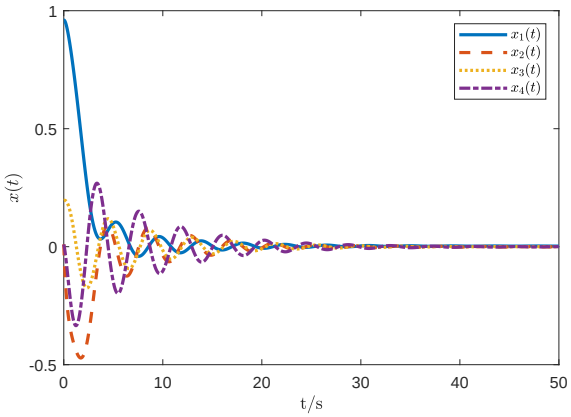

Figure 4. State responses with $\rho = 0$ by ETM.

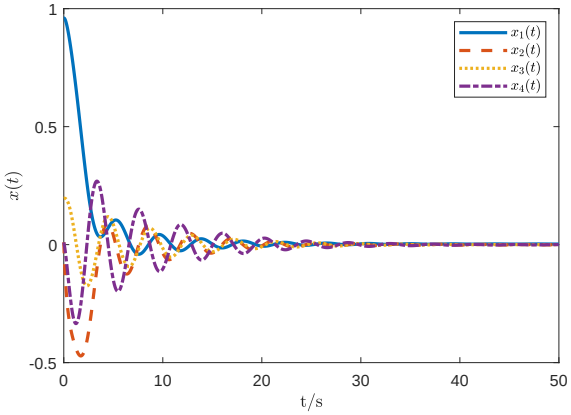

Figure 5. State responses with $\rho = 0.8$ by AETM.

When $\rho = 0$, AETM degrades to normal ETM with a fixed triggering parameter κ_0. But when $\rho = 0.8$, the triggering parameter $\kappa(l_m h)$ is dynamically adjusted with the fluctuation of the system state. And the change trajectories about $\kappa(l_m h)$ of $\rho = 0.8$ is illustrated in Figure 6. As shown in Figure 6, at the beginning of control, there exists a large error between the front and rear state. The parameter $\kappa(l_m h)$ fluctuates dramatically. When the system state gradually converges to zero, $\kappa(l_m h)$ is reaching to its maximum κ_{max}, which keeps a low transmitting frequency.

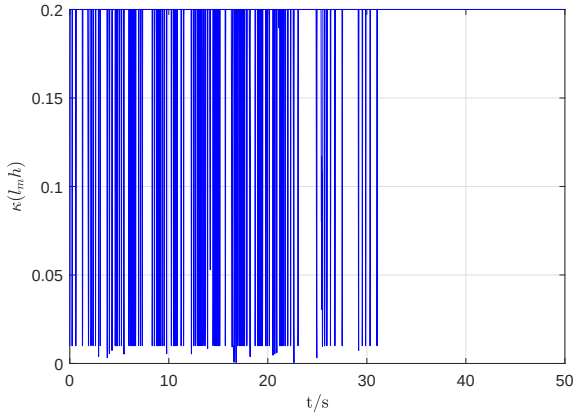

Figure 6. The dynamic parameters $\kappa(l_m k)$ with $\rho = 0.8$ by AETM.

Furthermore, Figures 7 and 8 show the triggering interval with regard to $\rho = 0, \rho = 0.8$. It is obvious that the triggering interval of $\rho = 0.8$ is bigger than $\rho = 0$. Therefore, the conclusions in Figures 7 and 8 are consistent with those in Table 1, which illustrates the effect of reducing network bandwidth occupancy of our proposed AETM ($\rho \neq 0$) is better than the traditional ETM ($\rho = 0$).

In this example, a single independent random variable $f_1(t)$ (with $\bar{f}_1 = 0.95, \quad \delta^2_{f1} = 0.05$) is taken to illustrate the random failure of the actuator in NCSs, which is assumed that $u^W(t) = f_1(t)u(t)$. That is to say, the control signal $u(t)$ arrives at the actuator, and after the processing of $u^W(t) = f_1(t)u(t)$, the control signal $u(t)$ becomes $u^W(t)$. From the above analysis, we can know $\rho = 0$ (traditional ETM) has a higher signal transmitting frequency than $\rho = 0.8$ (our proposed AETM). That is to say, the control signals $u(t)$ received by the actuator with $\rho = 0$ are more than that with $\rho = 0.8$. When the actuator receives the control signal, it will trigger $f_1(t)$ to generate a random value, which represents the actuator's fault. Thus, the probability of actuator faults triggering ($f_1(t)$) shown in Figure 10 fluctuates more intensively than that in Figure 9.

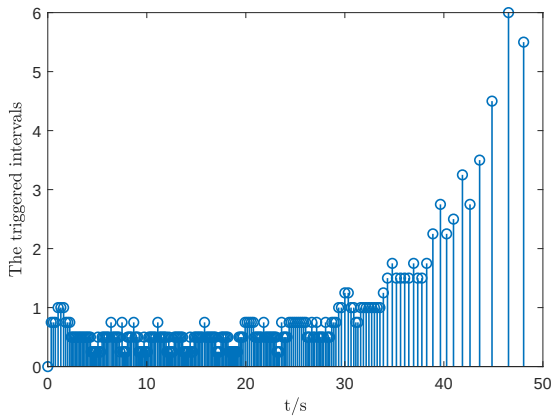

Figure 7. Event-triggered instants with $\rho = 0$ by ETM.

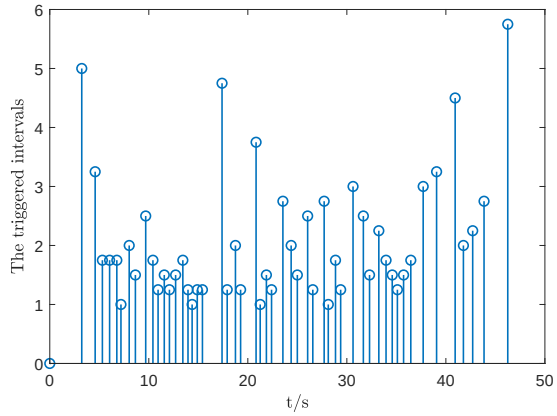

Figure 8. Event-triggered instants with $\rho = 0.8$ by AETM.

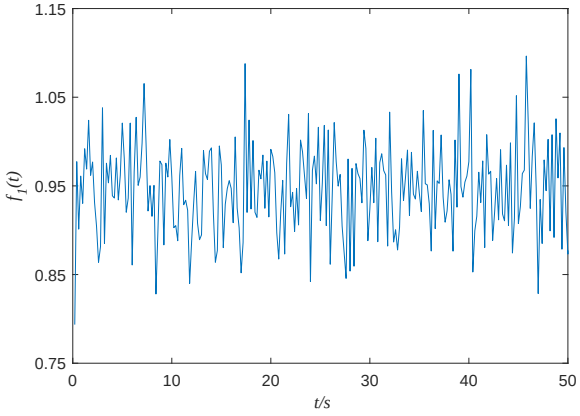

Figure 9. The probabilistic of actuator faults with $\rho = 0$ by ETM.

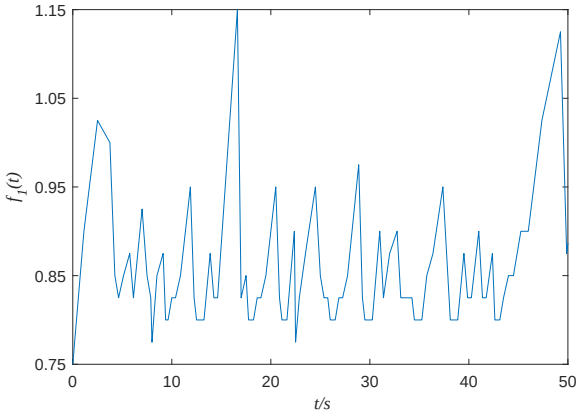

Figure 10. The probabilistic of actuator faults with $\rho = 0.8$ by AETM.

5. Conclusions

Considering actuator faults with AETM for NCSs, a novel event-triggered H_∞ reliable control approach is developed in this paper. First, the randomly occurring actuator faults are governed by a series of independent stochastic variables satisfying certain probability distributions. Then, according to the fluctuating trend of the current sampling state, the triggering threshold parameter is adaptively adjusted in the proposed AETM. As a result, the sampling-data model of NCSs considering AETM and actuator faults is constructed. Furthermore, a novel integral inequality is used to analyze the stability performance of H_∞ and derive the event-triggered H_∞ reliable control approach. In the end, case studies are presented to verify the effectiveness of the approach proposed in this paper. However, the security threats in actual communication networks are not considered in this paper, such as denial of service (DoS) attacks and deception attacks. The event-triggered reliable control approach considering various network attacks and actuator faults for NCSs will be the focus of our following work.

Acknowledgments

This work was supported by the National Natural Science Foundation of China under Grant (Nos. 61703060 and 12061088), the Sichuan Science and Technology Program under Grant Nos. 21YYJC0469 and 23ZDYF0645, the Project is funded by China Postdoctoral Science Foundation under Grant Nos. 2020M683274 and 2021T140092, Opening Fund of Geomathematics Key Laboratory of Sichuan Province (scsxdz2018zd04 and scsxdz2020zd01), the Open Research Project of Key Laboratory of Intelligent Manufacturing Quality Big Data Tracing and Analysis of Zhejiang Province, China Jiliang University Grant No. ZNZZSZ-CJLU2022-06.

Conflict of interest

The authors declare there is no conflicts of interest.

References

1. A. Bemporad, M. Heemels, M. Johansson, *Networked Control Systems*, Springer, London, 2010. https://doi.org/10.1007/978-0-85729-033-5
2. D. Zhang, P. Shi, Q. G. Wang, L. Yu, Analysis and synthesis of networked control systems: a survey of recent advances and challenges, *ISA Trans.*, **66** (2017), 376–392. https://doi.org/10.1016/j.isatra.2016.09.026
3. R. M. Murray, Future directions in control, dynamics, and systems: overview, grand challenges, and new courses, *Eur. J. Control*, **9** (2003), 144–158. Available from: http://users.cms.caltech.edu/ murray/preprints/mur03-ejc.pdf.
4. Y. Ma, Z. Q. Nie, S. L. Hu, Z. X. Li, R. Malekian, M. Sotelo, Fault detection filter and controller co-design for unmanned surface vehicles under dos attacks, *IEEE Trans. Intell. Transp. Syst.*, **22** (2021), 1422–1434. https://doi.org/10.1109/TITS.2020.2970472

5. X. Shang-Guan, Y. He, C. K. Zhang, L. Jin, W. Yao, L. Jiang, et al., Control performance standards-oriented event-triggered load frequency control for power systems under limited communication bandwidth, *IEEE Trans. Control Syst. Technol.*, **30** (2021), 860–868. https://doi.org/10.1109/TCST.2021.3070861

6. Q. S. Zhong, J. Yang, K. B. Shi, S. M. Zhong, Z. X. Li, M. A. Sotelo, Event-triggered H_∞ load frequency control for multi-area nonlinear power systems based on non-fragile proportional integral control strategy, *IEEE Trans. Intell. Transp. Syst.*, **23** (2021), 12191–12201. https://doi.org/10.1109/TITS.2021.3110759

7. C. Peng, J. Zhang, H. C. Yan, Adaptive event-triggering H_∞ load frequency control for network-based power systems, *IEEE Trans. Ind. Electron.*, **65** (2017), 1685–1694. https://doi.org/10.1109/TIE.2017.2726965

8. X. Shang-Guan, Y. He, C. Zhang, L. Jiang, J. W. Spencer, M. Wu, Sampled-data based discrete and fast load frequency control for power systems with wind power, *Appl. Energy*, **259** (2020), 114202. https://doi.org/10.1016/j.apenergy.2019.114202

9. K. Arora, A. Kumar, V. K. Kamboj, D. Prashar, S. Jha, B. Shrestha, et al., Optimization methodologies and testing on standard benchmark functions of load frequency control for interconnected multi area power system in smart grids, *Mathematics*, **8** (2020), 980. https://doi.org/10.3390/math8060980

10. K. Arora, A. Kumar, V. K. Kamboj, D. Prashar, B. Shrestha, G. P. Joshi, Impact of renewable energy sources into multi area multi-source load frequency control of interrelated power system, *Mathematics*, **9** (2021), 186. https://doi.org/10.3390/math9020186

11. L. Zhang, H. Gao, O. Kaynak, Network-induced constraints in networked control systemsa survey, *IEEE Trans. Ind. Inf.*, **9** (2012), 403–416. https://doi.org/10.1109/TII.2012.2219540

12. L. Hetel, C. Fiter, H. Omran, A. Seuret, E. Fridman, J. P. Richard, et al., Recent developments on the stability of systems with aperiodic samplingan overview, *Automatica*, **76** (2017), 309–335. https://doi.org/10.1016/j.automatica.2016.10.023

13. Y. H. Choi, S. J. Yoo, Quantized-feedback-based adaptive event-triggered control of a class of uncertain nonlinear systems, *Mathematics*, **8** (2020), 1603. https://doi.org/10.3390/math8091603

14. B. R. Xu, B. Li, Event-triggered state estimation for fractional-order neural networks, *Mathematics*, **10** (2022), 325. https://doi.org/10.3390/math10030325

15. P. Tabuada, Event-triggered real-time scheduling of stabilizing control tasks, *IEEE Trans. Autom. Control*, **52** (2007), 1680–1685. https://doi.org/10.1109/TAC.2007.904277

16. C. Peng, J. Zhang, Q. L. Han, Consensus of multi-agent systems with nonlinear dynamics using an intrgrated sampled-data-based event-triggered communication scheme, *IEEE Trans. Syst. Man Cybern.: Syst.*, **49** (2018), 589–599. https://doi.org/10.1109/TSMC.2018.2814572

17. D. Zhang, Q. L. Han, X. Jia, Network-based output tracking control for t-s fuzzy systems using an event-triggered communication scheme, *Fuzzy Sets Syst.*, **273** (2015), 26–48. https://doi.org/10.1016/j.fss.2014.12.015

18. C. Peng, S. Ma, X. Xie, Observer-based non-pdc control for networked t-s fuzzy systems with an event-triggered communication, *IEEE Trans. Cybern.*, **47** (2017), 2279–2287. https://doi.org/10.1109/TCYB.2017.2659698

19. Z. Wu, Y. Wu, Z. G. Wu, J. Lu, Event-based synchronization of heterogeneous complex networks subject to transmission delays, *IEEE Trans. Syst. Man Cybern.: Syst.*, **48** (2017), 2126–2134. https://doi.org/10.1109/TSMC.2017.2723760

20. X. M. Zhang, Q. L. Han, B. L. Zhang, An overview and deep investigation on sampled-data-based event-triggered control and filtering for networked systems, *IEEE Trans. Ind. Inf.*, **13** (2016), 4–16. https://doi.org/10.1109/TII.2016.2607150

21. W. P. M. H. Heemels, M. C. F. Donkers, A. R. Teel, Periodic event-triggered control for linear systems, *IEEE Trans. Autom. Control*, **58** (2012), 847–861. https://doi.org/10.1109/TAC.2012.2220443

22. C. Peng, M. Wu, X. Xie, Y. Wang, Event-triggered predictive control for networked nonlinear systems with inperfect premise matching, *IEEE Trans. Fuzzy Syst.*, **26** (2018), 2797–2806. https://doi.org/10.1109/TFUZZ.2018.2799187

23. S. Hu, D. Yue, L_2-gain analysis of event-triggered networked control systems: a discontinuous Lyapunov functional approach, *Int. J. Robust Nonlinear Control*, **23** (2013), 1277–1300. https://doi.org/10.1002/rnc.2815

24. E. Tian, C. Peng, Memory-based event-triggering H_∞ load frequency control for power systems under deception attacks, *IEEE Trans. Cybern.*, **50** (2020), 4610–4618. https://doi.org/10.1109/TCYB.2020.2972384

25. H. T. Sun, C. Peng, W. D. Zhang, T. C. Yang, Z. W. Wang, Security-based resilient event-triggered control of networked control systems under denial of service attacks, *J. Franklin Inst.*, **356** (2019), 10277–10295. https://doi.org/10.1016/j.jfranklin.2018.04.001

26. D. Yue, E. Tian, Q. L. Han, A delay system method for designing event-triggered controllers of networked control systems, *IEEE Trans. Autom. Control*, **58** (2012), 475–481. https://doi.org/10.1109/TAC.2012.2206694

27. S. Wen, X. Yu, Z. Zeng, J. Wang, Event-triggering load frequency control for multi-area power systems with communication delays, *IEEE Trans. Ind. Electron.*, **63** (2015), 1308–1317. https://doi.org/10.1109/TIE.2015.2399394

28. L. Dong, Y. Tang, H. He, C. Sun, An event-triggered approach for load frequency control with supplementary ADP, *IEEE Trans. Power Syst.*, **32** (2016), 581–589. https://doi.org/10.1109/TPWRS.2016.2537984

29. J. Yang, Q. S. Zhong, K. B. Shi, S. M. Shou, Co-design of observer-based fault detection filter and dynamic event-triggered controller for wind power system under dual alterable DoS attacks, *IEEE Trans. Inf. Forensics Secur.*, **17** (2022), 1270–1284. https://doi.org/10.1109/TIFS.2022.3160355

30. J. Yang, Q. S. Zhong, K. B. Shi, S. M. Shou, Dynamic-memory event-triggered H_∞ load frequency control for reconstructed switched model of power systems under hybrid attacks, *IEEE Trans. Cybern.*, 2022. https://doi.org/10.1109/TCYB.2022.3170560

31. S. Wang, X. Meng, T. Chen, Wide-area control of power systems through delayed network communication, *IEEE Trans. Control Syst. Technol.*, **20** (2011), 495–503. https://doi.org/10.1109/TCST.2011.2116022

32. Y. Q. Wang, G. F. Song, J. J. Zhao, J. Sun, G. M. Zhuang, Reliable mixed H_∞ and passive control for networked control systems under adaptive event-triggered scheme with actuator faults and randomly occurring nonlinear perturbations, *ISA Trans.*, **89** (2019), 45–57. https://doi.org/10.1016/j.isatra.2018.12.023

33. R. Sakthivel, S. Santra, K. Mathiyalagan, H. Y. Su, Robust reliable control design for networked control system with sampling conmmunication, *Int. J. Control*, **88** (2015), 2510–2522. https://doi.org/10.1080/00207179.2015.1048294

34. J. N. Li, Y. J. Pan, H. Y. Su, C. L. Wen, Stochastic reliable control of a class of networked control systems with actuator faults and input saturation, *Int. J. Control Autom. Syst.*, **12** (2014), 564–571. https://doi.org/10.1007/s12555-013-0371-7

35. W. Xue, P. Liu, S. Chen, Y. Huang, On extended state predictor observer based active disturbance rejection control for uncertain systems with sensor delay, in *2016 16th International Conference on Control, Automation and Systems (ICCAS)*, (2016), 1267–1271. https://doi.org/10.1109/ICCAS.2016.7832475

36. Ángel Cuenca, M. H. Zheng, M. Tomizuka, S. Sánchez, Non-uniform multi-rate estimator based periodic event-triggered control for resource saving, *Inf. Sci.*, **459** (2018), 86–102. https://doi.org/10.1016/j.ins.2018.05.038

37. W. Symens, H. van Brussel, J. Swevers, Gain-scheduling control of machine tools with varying structural flexibility, *CIRP Ann.*, **53** (2004), 321–324. https://doi.org/10.1016/S0007-8506(07)60707-0

38. C. Peng, T. C. Yang, Event-triggered communication and H_∞ control co-design for networked control systems, *Automatica*, **49** (2013), 1326–1332. https://doi.org/10.1016/j.automatica.2013.01.038

39. Y. L. Wang, Q. L. Han, Modelling and controller design for discrete-time networked control systems with limited channels and data drift, *Inf. Sci.*, **269** (2014), 332–348. https://doi.org/10.1016/j.ins.2013.12.041

40. H. Zhang, J. Yang, C. Y. Su, T-S fuzzy-model-based robust H_∞ design for networked control systems with uncertainties, *IEEE Trans. Ind. Inf.*, **3** (2007), 289–301. https://doi.org/10.1109/TII.2007.911895

41. L. Jin, Y. He, L. Jiang, A novel integral inequality and its application to stability analysis of linear system with multiple time delays, *Appl. Math. Lett.*, **124** (2022), 107648. https://doi.org/10.1016/j.aml.2021.107648

42. X. L. Zhu, G. H. Yang, Jensen inequality approach to stability analysis of discrete-time systems with time-varying delay, in *2008 American Control Conference*, (2008), 1644–1649. https://doi.org/10.1109/ACC.2008.4586727

43. A. Seuret, F. Gouaisbaut, Wirtinger-based integral inequality: application to time-delay systems, *Automatica*, **49** (2013), 2860–2866. https://doi.org/10.1016/j.automatica.2013.05.030

44. P. Park, W. I. Lee, S. Y. Lee, Auxiliary function-based integral/summation inequalities: application to continuous/discrete time-delay systems, *Int. J. Control Autom. Syst.*, **14** (2016), 3–11. https://doi.org/10.1007/s12555-015-2002-y

AIMS Press